

See discussions, stats, and author profiles for this publication at: <https://www.researchgate.net/publication/273453322>

# Kinetics of Distance-Dependent Recombination between Geminate Charge Carriers by Diffusion under Coulomb Interaction

ARTICLE in THE JOURNAL OF PHYSICAL CHEMISTRY C · FEBRUARY 2015

Impact Factor: 4.77 · DOI: 10.1021/acs.jpcc.5b00417

CITATIONS

2

READS

33

8 AUTHORS, INCLUDING:



**Rupashree Balia Singh**

National Institute of Advanced Industrial Sci...

27 PUBLICATIONS 424 CITATIONS

SEE PROFILE



**Hiroyuki Matsuzaki**

National Institute of Advanced Industrial Sci...

90 PUBLICATIONS 1,676 CITATIONS

SEE PROFILE



**Kazuhiko Seki**

National Institute of Advanced Industrial Sci...

86 PUBLICATIONS 928 CITATIONS

SEE PROFILE

# Kinetics of Distance-Dependent Recombination between Geminate Charge Carriers by Diffusion under Coulomb Interaction

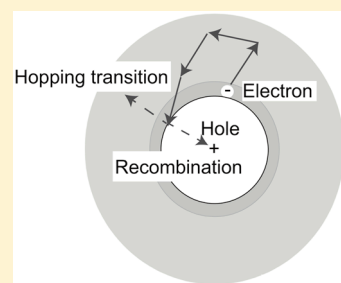
Yohichi Suzuki,<sup>†</sup> Akihiro Furube,<sup>†</sup> Rupashree Balia Singh,<sup>†</sup> Hiroyuki Matsuzaki,<sup>†</sup> Tsutomu Minegishi,<sup>‡</sup> Takashi Hisatomi,<sup>‡</sup> Kazunari Domen,<sup>‡,§</sup> and Kazuhiko Seki<sup>\*,†</sup>

<sup>†</sup>National Institute of Advanced Industrial Science and Technology (AIST), AIST Tsukuba Central 5, 1-1-1 Higashi, Tsukuba, Ibaraki 305-8565, Japan

<sup>‡</sup>Department of Chemical System Engineering, The University of Tokyo, 7-3-1 Hongo, Bunkyo-ku, Tokyo 113-8656, Japan

<sup>§</sup>Japan Technological Research Association of Artificial Photosynthetic Chemical Process (ARPChem), 5-1-5 Kashiwanoha, Kashiwa-shi, Chiba 277-8589, Japan

**ABSTRACT:** The survival probability of electron–hole pairs decays following a power law given by  $t^{-1/2}$  at long times when geminate recombination proceeds under diffusion and Coulomb interaction. Although the power law decay was known, the dependence of the decay amplitude on the strength of the Coulomb interaction, distance dependence of the intrinsic recombination rate, and the diffusion coefficient has not yet been fully understood. In this manuscript, we show analytical expressions on the amplitude of the asymptotic decay and compare the results with the overall kinetics obtained by numerical calculations. The results were applied to the measured data on the kinetics of carriers in LaTiO<sub>2</sub>N (LTON) solid photocatalyst measured using time-resolved diffuse reflectance spectroscopy (TRDR). The kinetic parameters of carriers were estimated and the presence of trap states was suggested. We also discuss the generalization of the results to the case that the diffusion is dispersive. The dispersive transport of carriers is considered to originate from the carrier transport by successive transitions among trap states with various release times.



## INTRODUCTION

Charge separation upon photoexcitation is an fundamental process in photovoltaic solar cells and photocatalytic activities.<sup>1–5</sup> Charge photogeneration is subsequently followed by recombination assisted by attractive Coulomb interaction. The recombination should be suppressed to have high photoconversion efficiency. It is also important to quantitatively characterize the recombination loss.

When semiconductors are excited with weak light pulses, generated charge carriers often decay with time following a power law with the exponent close to  $-1/2$ .<sup>1,6</sup> Moreover, when the photon energy is close to the band gap so that the energy in excess to that required to separate the geminate charge pair is small, the charge separation takes place by thermal motion of carriers from the initial small separation. The intrinsic recombination can be caused by tunneling between the electron and the hole.

When the pulsed light is irradiated using sufficiently long wavelength just enough to dissociate an electron and hole pair with an initial separation as small as possible, electron–hole pairs initially diffuse under the strong Coulomb interaction. In experiments, the survival probability of pairs can be measured.<sup>1,6–9</sup> The situation is often encountered when the transient densities of carriers are measured by pump–probe detection methods with band–edge excitations.<sup>1,6,7,9</sup> The seemingly simple geminate diffusion problem, however, turned out to be a hard theoretical problem for obtaining analytical expressions if the Coulomb interaction is present. The strength

of Coulomb interactions can be characterized by the Onsager radius defined by

$$r_c = \frac{e^2}{4\pi\epsilon_0 k_B T} \quad (1)$$

where  $e$ ,  $\epsilon$ ,  $\epsilon_0$ ,  $k_B$ , and  $T$  denote the elementary charge, dielectric constant, vacuum permittivity, Boltzmann constant, and temperature, respectively. When  $r_c$  is much larger than the closest possible distance of an electron–hole pair, the attractive Coulomb interaction between the hole and electron are larger than the thermal energy at the initial time after the charge pair generation. When the intrinsic recombination rate is small and charge pairs separate from close separation distance, the survival probability of pairs are very much affected by the distance dependence of the intrinsic recombination rate at small separation distance. To quantify the survival probability, we explicitly take into account the distance dependence of the intrinsic recombination rate. Even under the attractive Coulomb interaction, some fraction of the pairs may escape recombination by thermal diffusion if the intrinsic recombination rate is small. When we analyze experimental results, we show that overall decay is affected by the Coulomb interaction and the closest separation distance of an electron–hole pair.

**Received:** January 15, 2015

**Revised:** February 19, 2015

In the presence of Coulomb interaction, analytical asymptotic solution was obtained when reaction occurs at some distance. For distance-dependent reactions, approximate methods have been developed.<sup>10–12</sup> However, each method has its limitation in the applicability with respect to the initial separation distance, the value of  $r_0$ , and the distance-dependence of the intrinsic recombination rate,  $k(r)$ . In this manuscript, we mainly study the case when the initial distance is equal to the closest separation distance  $R$  expressed by the reflecting boundary condition;  $R$  could be given by the lattice constant if carriers execute random walks. In some works, a perfectly absorbing boundary condition was imposed at a certain separation distance between an electron and a hole.<sup>6,13</sup> As in our previous article, we assume that recombination occurs exclusively by the intrinsic rate and imposes a perfectly reflecting boundary condition at the closest separation distance denoted by  $R$ .<sup>10,11</sup> Previously, the diffusion-controlled recombination of the geminate pair was studied even when the diffusion was dispersive though in the absence of Coulomb interaction.<sup>10,11</sup> The dispersive transport of carriers can be measured, for example by the transient current in the time-of-flight experiments and is expressed by the time evolution of mean-square displacements,  $\langle r(t)^2 \rangle \sim t^\alpha$  with  $\alpha < 1$ .<sup>14,15</sup> The carrier transport becomes dispersive when carriers execute hopping transitions with a distributed release times. In this paper, we study the effect of both the dispersive diffusion and Coulomb interaction on tunneling recombination.

To apply the above-mentioned theory to estimate the diffusion coefficients from the experimental data, we closely examine the robustness of the values of the diffusion coefficients estimated from the asymptotic decay against the change in the initial distance and the attenuation factor of intrinsic recombination rate showing the distance dependence.

As an illustration, we study recent experimental data on the transient decay of carriers in the oxynitride LaTiO<sub>2</sub>N (LTON). LTON has a potential to absorb visible light of 600 nm (bandgap of 2.1 eV),<sup>8,9</sup> and is a photocatalyst for generating H<sub>2</sub> and O<sub>2</sub> from water. By analyzing the asymptotic decay profile of carriers in LTON, measured by time-resolved diffuse reflectance spectroscopy (TRDR), the diffusion coefficient of carriers is estimated. We note from the results of numerical calculations that the overall decay kinetics is sensitive to the closest separation distance of an electron-hole pair in the presence of Coulomb interaction. The closest separation distance of an electron-hole pair is estimated by comparison between the experimental decay profile and the overall decay obtained by numerical calculations.

## ■ FORMAL EXPRESSIONS OF SURVIVAL PROBABILITY

The geminate recombination processes are schematically shown in Figure 1. The initial separation between an electron and a hole is denoted by  $r_0$ . We take into account Coulomb interaction between an electron and a hole. The electron undergoes random walks. Although both the electron and the hole may move, the diffusive motion of carriers are taken into account by assuming an immobile hole and a mobile electron with the relative diffusion coefficient denoted by  $D$ . The recombination takes place according to the distance between the electron and the hole denoted by  $r$  and the distance-dependent rate is expressed by  $k(r)$ .

When a pair of positive and negative charge carriers with initial separation denoted by  $r_0$  exhibits Brownian motion under

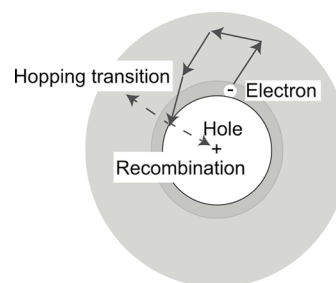


**Figure 1.** Initial distance between an electron and a hole is denoted by  $r_0$ . The strength of Coulomb interaction between an electron and a hole is indicated by gray levels. The electron executes random walks under the Coulomb interaction outside the spherical region of radius  $R$  and the relative diffusion coefficient is denoted by  $D$ . The closest separation distance of an electron and a hole is denoted by  $R$ . The electron-hole recombination takes place with the distance-dependent rate denoted by  $k(r)$ .

the Coulomb interaction, the probability of finding a pair of carriers with separation  $r$  at time  $t$  is obtained by solving

$$\frac{\partial}{\partial t} p(r, t|r_0) = \mathcal{L}p(r, t|r_0) - k(r)p(r, t|r_0) \quad (2)$$

where  $\mathcal{L}$  is the operator expressed as

$$\mathcal{L} = D \frac{1}{r^2} \frac{\partial}{\partial r} r^2 e^{-U(r)} \frac{\partial}{\partial r} e^{U(r)} \quad (3)$$

and  $U(r) = -|r_c|/r$ . In the above,  $D$  denotes the relative diffusion coefficient of the geminate pair, and  $k(r)$  denotes the intrinsic recombination rate. For tunneling recombination,  $k(r)$  can be expressed as  $k(r) = k_0 \exp(-2\beta r)$ , where  $\beta$  is the attenuation factor of tunneling. To take into account the closest separation distance of a pair, we introduce a reflecting boundary condition at a separation distance represented by  $R$  (see Figure 1):

$$\frac{\partial}{\partial r} e^{U(r)} p(r, t|r_0)|_{r=R} = 0 \quad (4)$$

In the Laplace domain, the Green function for the operator given by eq 3 can be expanded in terms of  $|r_c|(s/D)^{1/2}$  and the lowest order results can be expressed as<sup>16–19</sup>

$$\hat{G}(r, s|r_0) = \frac{\exp(|r_c|/r)}{4\pi D|r_c|} \left[ 1 - \exp\left(-\frac{|r_c|}{\max(r_0, r)}\right) - |r_c| \sqrt{\frac{s}{D}} \right] \quad (5)$$

where  $\max(\cdot, \cdot)$  denotes the maximum of the arguments. The pair survival probability with initial separation given by  $r_0$  is defined by

$$S_0(r_0, t) = 4\pi \int_R^\infty r^2 dr p(r, t|r_0) \quad (6)$$

The Laplace transformation of  $S(r_0, t)$  is obtained by the lowest order perturbation expansion with respect to  $k(r)$  as,

$$\hat{S}(r_0, s) = (1 - \kappa_1(r_0, s))/s \quad (7)$$

where  $\kappa_1(r_0, s)$  is defined as

$$\kappa_1(r_0, s) = 4\pi \int_R^\infty r^2 dr k(r) \hat{G}(r, s|r_0) \quad (8)$$

Using the Padé approximant, the survival probability in the Laplace domain is obtained as<sup>20</sup>

$$\hat{S}_p(r_0, s) = \frac{1}{s} \left[ 1 - \frac{\hat{\kappa}_1(r_0, s)^2}{\hat{\kappa}_1(r_0, s) + \hat{\kappa}_2(r_0, s)} \right] \quad (9)$$

where  $\hat{\kappa}_2(r_0, s)$  is given by

$$\hat{\kappa}_2(r_0, s) = (4\pi)^2 \int_R r_1^2 dr_1 \int_R r_2^2 dr_2 k(r_1) k(r_2) \hat{G}(r_1, s/r_2) \hat{G}(r_2, s/r_1) \quad (10)$$

Below, the formal result given by eq 9 will be evaluated using the inverse Laplace transformation and the asymptotic decay will be obtained.

## DECAY KINETICS OF GEMINATE CHARGE PAIRS

The asymptotic solution of the survival probability is obtained by substituting eq 5 into eq 7 and expanding the result in terms of  $|r_c|/D$  for the lowest order perturbative solution. By noticing that the inverse Laplace transformation of  $1/s^{1/2}$  is  $1/(\pi t)^{1/2}$ , the lowest order perturbative solution for the case that the initial separation is at the closest distance is obtained as

$$S_0(R, t) = 1 - \kappa_D K_p(R, \infty) + \kappa_D K_c(R, \infty) \frac{|r_c|}{\sqrt{\pi D t}} \quad (11)$$

where we defined

$$\kappa_D = \frac{k_0 |r_c|^2}{D} \quad (12)$$

$$K_p(r_1, r_2) = \frac{1}{|r_c|^3} \int_{r_1}^{r_2} r^2 dr \frac{k(r)}{k_0} [\exp(|r_c|/r) - 1] \quad (13)$$

$$K_c(r_1, r_2) = \frac{1}{|r_c|^3} \int_{r_1}^{r_2} r^2 dr \frac{k(r)}{k_0} \exp(|r_c|/r) \quad (14)$$

The corresponding result for the Padé approximant is obtained from eq 9 as

$$S_p(R, t) = 1 - \frac{\kappa_D K_p(R, \infty)}{1 + \kappa_D (K_c(R, \infty) - h_0)} + \frac{\{ \kappa_D K_c(R, \infty) [1 + \kappa_D (2K_c(R, \infty) - K_p(R, \infty))] - \kappa_D^2 [2K_c(R, \infty) h_0 + h_r] \}}{[1 + \kappa_D (K_c(R, \infty) - h_0)]^2} \times \frac{|r_c|}{\sqrt{\pi D t}} \quad (15)$$

$$\approx 1 - \frac{\kappa_D K_p(R, \infty)}{1 + \kappa_D K_c(R, \infty)} + \frac{\kappa_D K_c(R, \infty)}{[1 + \kappa_D K_c(R, \infty)]^2} \frac{|r_c|}{\sqrt{\pi D t}} \quad (16)$$

where we defined

$$h_0 = \frac{1}{|r_c|^3 K_p(R, \infty)} \int_R r^2 dr \frac{k(r)}{k_0} [K_p(R, r) + \exp(|r_c|/r) K_m(r, \infty)] \quad (17)$$

$$h_r = \frac{1}{|r_c|^3} \int_R r^2 dr \frac{k(r)}{k_0} [\exp(|r_c|/r) K_p(r, \infty) + (\exp(|r_c|/r) - 1) K_c(R, r)] \quad (18)$$

and

$$K_m(r_1, r_2) = \frac{1}{|r_c|^3} \int_{r_1}^{r_2} r^2 dr \frac{k(r)}{k_0} (1 - \exp(-|r_c|/r)) \quad (19)$$

In deriving eq 16 from eq 15, we assumed  $R/r_c \ll 1$ . As a consequence,  $K_p(R, \infty)$  and  $h_r$  are close to  $K_c(R, \infty)$ , and they are larger than  $h_0$ .

As shown below, eq 16 is a reasonably simple expression. When the recombination occurs by tunneling, eq 16 can be expressed by analytical functions using  $\int_R r^2 dr \exp(-2\beta r) = (1 + 2R\beta + 2R^2\beta^2) \exp(-2\beta R)/(4\beta^3)$  and

$$\begin{aligned} \int_R^\infty r^2 dr \exp(-2\beta r + |r_c|/r) \\ = |r_c|^3 \sum_{j=0}^{\infty} \frac{(2\beta |r_c|)^{j-3}}{j!} \Gamma(3-j, 2\beta R) \end{aligned} \quad (20)$$

where  $\Gamma(a, x) = \int_x^\infty dt t^{a-1} \exp(-t)$  is the incomplete Gamma function.<sup>21</sup>

The above results are obtained approximately by focusing on the asymptotic decay of the pair survival probability. The overall decay can be calculated numerically. We calculate the numerical results by solving the differential equation satisfied by the pair survival probability. In the Laplace domain, the pair survival probability with the initial separation  $r$  satisfies<sup>22,23</sup>

$$s\hat{S}(r, s) - 1 = D \frac{1}{r^2} e^{U(r)} \frac{\partial}{\partial r} r^2 e^{-U(r)} \frac{\partial}{\partial r} \hat{S}(r, s) - k(r) \hat{S}(r, s) \quad (21)$$

where the perfectly reflecting boundary condition is imposed,

$$\left. \frac{\partial}{\partial r} \hat{S}(r, s) \right|_{r=R} = 0 \quad (22)$$

The numerical results of the pair survival probability are obtained using the Stehfest method for the inverse Laplace transformation combined with the numerical solution of eq 21 obtained using the finite difference method implemented in Mathematica.<sup>24–26</sup> The results are plotted in Figures 2–4 by closed squares.

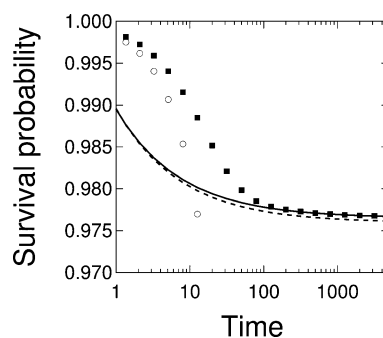


**Figure 2.** Survival probability as a function of dimensionless time given by  $tD/|r_c|^2$  for  $\epsilon = 9.0$ ,  $R = 0.5$  nm,  $D = 10^{-3}$  cm<sup>2</sup>/s, and  $k_0 |r_c|^2/D = 0.005$ , and  $\beta = 1$  nm<sup>-1</sup>. The closed squares denote the numerical exact results calculated by eq 21. The solid line, dashed line, and circles indicate the results of Padé approximant given by eq 15, the lowest order approximation given by eq 11, and the static reaction approximation given by eq 23, respectively.

We also plotted the result by assuming static reaction without any movement of geminate pairs,

$$S_s(R, t) = \exp(-k(R)t) \quad (23)$$

in Figures 2–4 by circles. As expected, the initial decay follows the static reaction only at short times characterized by  $tD/|r_c|^2$

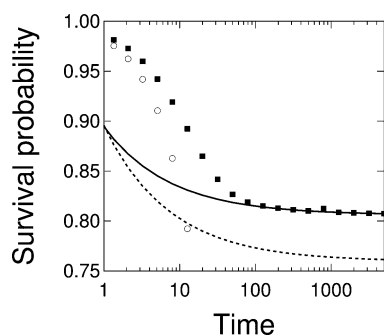


**Figure 3.** Survival probability as a function of dimensionless time given by  $tD/|r_c|^2$ .  $k_0 |r_c|^2/D = 0.05$  and the other parameter values are the same as those in Figure 2. The closed squares denote the numerical exact results calculated by eq 21. The solid line, dashed line, and circles indicate the results of Padé approximant given by eq 15, the lowest order approximation given by eq 11, and the static reaction approximation given by eq 23, respectively.

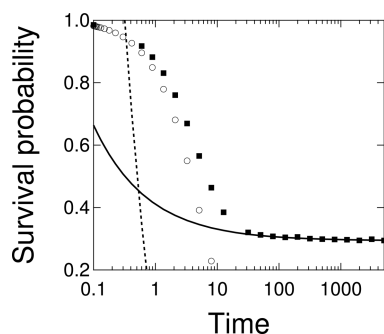


**Figure 4.** Survival probability as a function of dimensionless time given by  $tD/|r_c|^2$ .  $k_0 |r_c|^2/D = 0.5$  and the other parameter values are the same as those in Figure 2. The closed squares denote the numerical exact results calculated by eq 21. The solid line, dashed line, and circles indicate the results of Padé approximant given by eq 15, the lowest order approximation given by eq 11, and the static reaction approximation given by eq 23, respectively.

$\leq 1$ , regardless of the amplitude of the intrinsic recombination rate.

In Figures 2–4, the results of the lowest order approximation and Padé approximant are compared to the exact numerical results. The lowest order approximation given by eq 11 reproduces the numerical results only when the intrinsic recombination rate is small and the ultimate probability of separation in the limit of  $t \rightarrow \infty$  is larger than 0.9. In contrast, the results of Padé approximant are fairly good as long as the asymptotic decay is concerned. Even for the relatively large values of the intrinsic recombination rate used to draw Figure 4, the asymptotic decay obtained from eq 15 reproduces the numerical results. Although Padé approximant is accurate, the expression is given by the double spatial integration and is rather complicated. Equation 16 is obtained by further simplifying eq 15 and is expressed only by the single spacial integration. The results of eq 16 overlapped with the solid lines obtained from eq 15 in Figures 2–4.

By decreasing the value of  $\beta$  to 1/10 of that in Figures 2–4, the results of eq 16 deviate from that of eq 15 when the intrinsic recombination rate is large (results not shown). We note that the values obtained using eq 16 are larger than those obtained using eq 15. Even under the long-range reactivity, the

results of full Padé approximant given by eq 15 reproduce the asymptotic decay of numerical results.

## METHOD FOR ANALYZING EXPERIMENTAL RESULTS

According to eq 16, the ultimate survival probability can be expressed as

$$S_\infty = 1 - \frac{\kappa_D K_p(R, \infty)}{1 + \kappa_D(K_c(R, \infty) - h_0)} \approx 1 - \frac{\kappa_D K_p(R, \infty)}{1 + \kappa_D K_c(R, \infty)} \quad (24)$$

where  $\kappa_D = k_0 |r_c|^2/D$  is defined by eq 12. To analyze experimental results, it is convenient to rewrite eq 24 as

$$\kappa_D = \frac{1 - S_\infty}{(K_c(R, \infty) - h_0)S_\infty + K_p - K_c(R, \infty) + h_0} \quad (25)$$

$$\approx \frac{1 - S_\infty}{K_c(R, \infty)S_\infty + K_p - K_c(R, \infty)} \quad (26)$$

When the dielectric constants,  $R$  and  $k(r)$ , are known, the value of  $\kappa_D$  can be estimated from the ultimate survival probability using eq 25 or eq 26. The ultimate survival probability can be obtained from the transient decay if we know the initial absorbance and the residual absorbance by the remaining carriers in the sample at long times.

Equation 16 can be expressed as

$$S_p(R, t) = S_\infty(R) + \frac{\kappa_D K_c(R, \infty)}{[1 + \kappa_D K_c(R, \infty)]^2} \frac{|r_c|}{\sqrt{\pi D t}} \quad (27)$$

By fitting the asymptotic decay to  $1/t^{1/2}$  time dependence, the decay amplitude is obtained. The relative diffusion coefficient can be obtained from the decay amplitude using the value of  $\kappa_D$  estimated by eq 25 or eq 26.

## EFFECT OF INITIAL SEPARATION

In experiments, the initial separation may be different from the closest separation distance of an electron-hole pair and distributed. In this section, we generalize the above method to estimate the values of diffusion coefficients from the asymptotic decay of the pair survival probability for an arbitrary initial distance. We will show that the values of diffusion coefficients can be estimated even without the precise knowledge of the initial separation.

The asymptotic decay of the pair survival probability can be obtained from eq 9 for general initial separation as

$$S_p(r_0, t) = S_\infty(r_0) + S_t(r_0) \frac{|r_c|}{\sqrt{\pi D t}} \quad (28)$$

$S_\infty(r_0)$  is expressed as

$$S_\infty(r_0) = 1 - \frac{\kappa_D K_1(r_0)^2}{K_1(r_0) + \kappa_D K_2(r_0)} \quad (29)$$

where we defined,

$$K_i(r_0) = \frac{1}{|r_c|^3} \int_R^\infty r^2 dr \frac{k(r)}{k_0} \exp\left(\frac{|r_c|}{r}\right) \times \left[1 - \exp\left(\frac{-|r_c|}{\max(r, r_0)}\right)\right] \quad (30)$$



$$K_2(r_0) = \frac{1}{|r_c|^6} \int_R^\infty r^2 dr \int_R^\infty r_1^2 dr_1 \frac{k(r)}{k_0} \frac{k(r_1)}{k_0} \times \exp\left(\frac{|r_c|}{r} + \frac{|r_c|}{r_1}\right) \times \left[1 - \exp\left(\frac{-|r_c|}{\max(r, r_1)}\right)\right] \times \left[1 - \exp\left(\frac{-|r_c|}{\max(r_1, r_0)}\right)\right] \quad (31)$$

$S_t(r_0)$  is expressed as

$$S_t(r_0) = \frac{\kappa_D K_1(r_0) [(2\kappa_D K_2(r_0) + K_1(r_0)) K_c(R, \infty) - \kappa_D K_1(r_0) L_2(r_0)]}{[K_1(r_0) + \kappa_D K_2(r_0)]^2} \quad (32)$$

where  $K_c(R, \infty)$  was defined by eq 14 and we defined

$$L_2(r_0) = \frac{1}{|r_c|^6} \int_R^\infty r^2 dr \int_R^\infty r_1^2 dr_1 \frac{k(r)}{k_0} \frac{k(r_1)}{k_0} \times \exp\left(\frac{|r_c|}{r} + \frac{|r_c|}{r_1}\right) \times \left[2 - \exp\left(\frac{-|r_c|}{\max(r, r_1)}\right) - \exp\left(\frac{-|r_c|}{\max(r_1, r_0)}\right)\right] \quad (33)$$

When  $r_0 > R$ , eq 25 is generalized to

$$\kappa_D = \frac{K_1(r_0) [1 - S_\infty(r_0)]}{K_2(r_0) S_\infty(r_0) + K_1(r_0)^2 - K_2(r_0)} \quad (34)$$

$\kappa_D$  is proportional to the strength of the intrinsic recombination rate given by  $k_0$ . For a given value of  $S_\infty(r_0)$ ,  $\kappa_D$  is sensitive to the initial distance given by  $r_0$ . The ultimate pair survival probability increases with increasing initial distance. Therefore, the value of  $k_0$  should be larger when the initial distance is larger for the same value of the ultimate pair survival probability.

In experiments, we often observe  $S_\infty(r_0)$  without information on the initial distance. When the normalized decay amplitude defined by

$$N_t(r_0) = \frac{S_t(r_0)}{S_\infty(r_0)} \quad (35)$$

is insensitive to  $r_0$ , the value of the diffusion coefficient can be estimated from the asymptotic decay using the measured value of  $S_\infty(r_0)$  without affected by  $r_0$ ; eq 28 can be rewritten as

$$S_p(r_0, t) = S_\infty(r_0) \left(1 + N_t(r_0) \frac{|r_c|}{\sqrt{\pi D t}}\right) \quad (36)$$

and if  $N_t(r_0)$  is insensitive to  $r_0$  the value of  $D$  is obtained from the amplitude of power law decay with the exponent  $-1/2$  by assuming  $r_0 = R$ .

In Figures 5 and 6, we show  $1/N_t(r_0)$  as a function of  $\kappa_D$  for various values of  $r_0$ . We also study the effect of the values of  $\beta$  which is the attenuation factor of tunneling. When  $\beta = 1 \text{ nm}^{-1}$  and  $r_c = 6.2 \text{ nm}$  ( $\epsilon = 9$ ),  $1/N_t(r_0)$  increases linearly by increasing  $1/\kappa_D$ . In Figure 5, the results for  $r_0/r_c = 0.081$  (0.5 nm), 0.65 (4 nm) overlap.  $N_t(r_0)$  is insensitive to the values of  $r_0$  as long as  $\beta > 1/r_c$  is satisfied.  $1/[1 - S_\infty(r_0)]$  also increases by increasing  $1/\kappa_D$ , but it shows  $r_0$  dependence. For any value of  $r_0$ ,  $N_t(r_0)$  converges to the value close to 1 as  $1/\kappa_D$  is decreased ( $\kappa_D$  is increased).

Different  $\kappa_D$  dependence can be found for  $N_t(r_0)$  when  $\beta = 0.1 \text{ nm}^{-1}$  and  $r_c = 6.2 \text{ nm}$  ( $\epsilon = 9$ ).  $N_t(r_0)$  increases beyond the value of 1 with increasing  $\kappa_D$ . When  $N_t(r_0) < 1$  all lines for different values of  $r_0/r_c$  overlap but they differ when  $N_t(r_0) > 1$ . The value of  $\beta$  indicates extremely long-range reactivity satisfying  $\beta r_c < 1$ . Reaction globally interferes with diffusional flow under Coulomb interaction. Under such circumstances,  $N_t(r_0)$  increases beyond the value of 1 and have different values

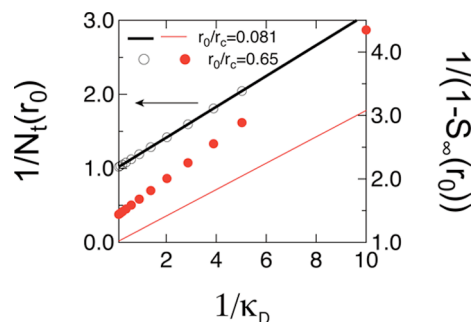


**Figure 5.**  $1/N_t(r_0)$  and  $1/[1 - S_\infty(r_0)]$  plotted against  $1/\kappa_D$ .  $\beta = 1 \text{ nm}^{-1}$ ,  $\epsilon = 9$ , and  $R = 0.5 \text{ nm}$ . The thick and (red) thin solid lines indicate  $1/N_t(r_0)$  and  $1/[1 - S_\infty(r_0)]$  for  $r_0 = 0.5 \text{ nm}$  ( $r_0/r_c = 0.081$ ), respectively. The open and (red) closed circles indicate  $1/N_t(r_0)$  and  $1/[1 - S_\infty(r_0)]$  for  $r_0 = 4 \text{ nm}$  ( $r_0/r_c = 0.65$ ), respectively.

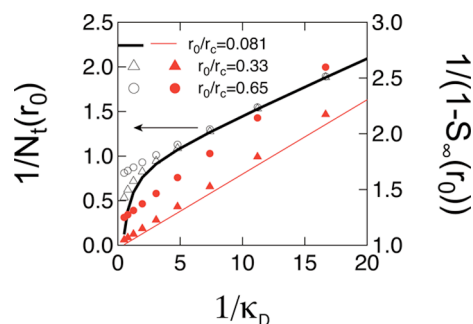


**Figure 6.**  $1/N_t(r_0)$  and  $1/[1 - S_\infty(r_0)]$  plotted against  $1/\kappa_D$ .  $\beta = 0.1 \text{ nm}^{-1}$ ,  $\epsilon = 9$ , and  $R = 0.5 \text{ nm}$ . The thick and (red) thin solid lines indicate  $1/N_t(r_0)$  and  $1/[1 - S_\infty(r_0)]$  for  $r_0 = 0.5 \text{ nm}$  ( $r_0/r_c = 0.081$ ), respectively. The open and (red) closed triangles indicate  $1/N_t(r_0)$  and  $1/[1 - S_\infty(r_0)]$  for  $r_0 = 2 \text{ nm}$  ( $r_0/r_c = 0.33$ ), respectively. The open and (red) closed circles indicate  $1/N_t(r_0)$  and  $1/[1 - S_\infty(r_0)]$  for  $r_0 = 4 \text{ nm}$  ( $r_0/r_c = 0.65$ ), respectively.

depending on  $r_0$ .  $1/[1 - S_\infty(r_0)]$  also increases by increasing  $1/\kappa_D$  and it shows  $r_0$  dependence, as in the case of  $\beta = 1 \text{ nm}^{-1}$ .

It should be reminded that  $N_t(r_0) = 1/[1 - \exp(-|r_c|/R)] \approx 1$  is satisfied for a contact reaction expressed by

$$k(r) = \kappa_L \delta(r - R) / (4\pi R^2) \quad (37)$$

in the limit of  $k_L \rightarrow \infty$ .<sup>22,27,28</sup>  $\kappa_D$  is proportional to  $k_L$  for a contact reaction and  $1/[1 - S_\infty(r_0)]$  increases linearly by increasing  $1/\kappa_D$  for a contact reaction. For a contact reaction,  $1/N_t(r_0)$  increases linearly with increasing  $1/\kappa_D$  from the limiting value of  $1/N_t(r_0) \approx 1$  at  $1/\kappa_D \rightarrow 0$  and the results are similar to Figure 5. In Figure 6,  $1/N_t(r_0)$  deviates from linear  $1/\kappa_D$  dependence when  $1/\kappa_D$  is close to zero. In this region,  $1/N_t(r_0)$  depends on the initial separation. The intrinsic reaction rate is long-ranged in Figure 6 compared to that in Figure 5. Both the sensitivity of  $N_t(r_0)$  to initial distance and the breakdown of the linear relation are related to the interference between diffusion and reaction for long-range reactivity expressed by  $\beta r_c < 1$ .

$S_t(r_0)$  in eq 28 can be very simplified for  $R = r_0$ , as shown in eq 27. When the values of  $r_c$ ,  $S_\infty(r_0)$  and the amplitude of  $1/t^{1/2}$  dependence of the survival probability were obtained from experiments, we can estimate  $D$  using eq 28 by calculating  $S_t(r_0)$  for arbitrary chosen value of  $r_0$  if  $N_t(r_0) = S_t(r_0)/S_\infty(r_0)$  is insensitive to  $r_0$ .  $N_t(r_0)$  is insensitive to  $r_0$  when  $\beta r_c > 1$  and  $r_0 = R$  is the most convenient choice for the calculation. We stress that the value of diffusion constant can be estimated when  $\beta r_c >$

1 using the simple analytical expression for  $S_i(r_0)$  obtained by assuming  $r_0 = R$ . The realistic values of  $\beta$  satisfy  $\beta r_c > 1$  since  $r_c = 5\text{--}6\text{ nm}$  can be estimated from the typical values of the dielectric constants of the semiconductor materials given by  $\epsilon \sim 10$ . If the ultimate survival probability is small corresponding to the large values of  $\kappa_D$ , the diffusion constant can be roughly estimated by setting  $N_i(r_0) = 1$  using eq 36.

## RECOMBINATION KINETICS IN LaTiO<sub>2</sub>N (LTON) PHOTOCATALYST

**Analysis of Experimental Data.** The above theoretical results can be applied to experimental results to understand the loss mechanism of long-lived carriers. We have already performed primitive analysis to the experimental data of carrier concentrations in LaTiO<sub>2</sub>N (LTON) photocatalyst probed by Subns-Time-Resolved Diffuse Reflectance (TRDR).<sup>9</sup> TRDR is a powerful method to measure the carrier concentration when the sample is not transparent.<sup>29–32</sup> In the recent experiment using weak excitation light pulses, the absorbance immediately after the excitation was proportional to the light intensity and the decay was not affected by the light intensity. The decay of absorbance in nanosecond time regime exhibited a power law dependence with the exponent  $-1/2$  and was interpreted as the diffusion-controlled geminate recombination of an electron-hole pair.<sup>9</sup>

In experiments, the extracted value of the ultimate survival probability is  $S_\infty = 0.047$ . The absorbance is proportional to the number of carriers remained and thus is proportional to the survival probability of carriers. For simplicity, the absorbance measured using TRDR will be referred to as survival probability. In Figure 7, the measured data beyond 0.1 ns

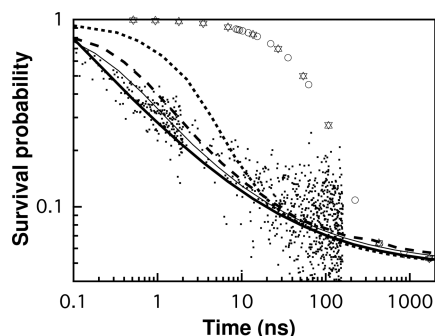


**Figure 7.** Thick solid line indicates  $0.047 + 0.234/(t[\text{ns}])^{1/2}$  obtained by fitting to eq 36. Triangles, circles, and inverted triangles denote the full decay curves obtained by the numerical inverse Laplace transformation of eq 21 with  $\beta = 0.5, 1$ , and  $2\text{ nm}^{-1}$  when  $r_0 = R = 0.5\text{ nm}$ , respectively. They give essentially the same results. The short dashed line, long dashed line, and thin solid line indicate the full decay curves obtained using eq 21 for  $\beta = 1\text{ nm}^{-1}$  when  $r_0 = R = 1\text{ nm}$ ,  $r_0 = R = 5\text{ nm}$ , and  $r_0 = R = 10\text{ nm}$ , respectively.

decay along a power-law function with the exponent  $-1/2$ . In this time regime, the measured data can be regarded as the asymptotic decay. We roughly estimate the value of the diffusion constant using eq 36 with  $N_i(r_0) = 1$  by noticing the small value of the ultimate survival probability. The relative dielectric constant of the sample is 8.91.<sup>8</sup> By employing eq 36 with  $N_i(r_0) = 1$ , the diffusion constant was estimated to be  $5 \times 10^{-6}\text{ cm}^2/\text{s}$ .

To confirm the above estimation, we analyze the experimental results using eqs 26 and 27. We assume  $R = 0.5$

nm taken from the typical value of the lattice constant of semiconductors. By assuming  $\beta = 1\text{ nm}^{-1}$ , we obtained  $\kappa_D = 3.9$  using eq 26. By substituting the value of  $\kappa_D$  in eq 27, we got  $D = 4.5 \times 10^{-6}\text{ cm}^2/\text{s}$ . By assuming  $\beta = 0.5\text{ nm}^{-1}$ , we obtained  $\kappa_D = 2.1$  and  $D = 4.5 \times 10^{-6}\text{ cm}^2/\text{s}$ . The value is close to that roughly estimated using eq 36 with  $N_i(r_0) = 1$ . As shown in the preceding section, the estimated value of diffusion coefficient is not affected by the assumed values of the initial separation, although the ultimate survival probability depends on the initial separation.

So far, we have estimated the values of the diffusion coefficients from the asymptotic decay of the survival probability. In Figure 7, we investigate whether the asymptotic decay can be found within the time region of experiments using the full decay curve obtained by the numerical inverse Laplace transformation of eq 21 with the reasonable values of parameters. The experimental data of ref 9 were shown by dots. When we use  $R = 0.5\text{ nm}$  taken from the typical value of the lattice constant of semiconductors, the decay curves were given by triangles, circles and inverted triangles for  $\beta = 0.5, 1$ , and  $2$ , respectively. All these three results were essentially the same and drawn using initial separation of  $r_0 = 0.5\text{ nm}$ . By increasing the initial separation, the decay is delayed. Compared to the decay of experimental data, the theoretical asymptotic decay is delayed even when the initial separation is equal to  $R$ . The faster decay is not obtained by merely changing  $\beta$ -values and  $r_0$  values.

In the same figure, we show the full decay curves when the value of  $R$  is increased from  $R = 0.5\text{ nm}$ . The values of  $\kappa_D$  and  $D$  were obtained by using eqs 26 and 27 together with  $0.047 + 0.234/(t[\text{ns}])^{1/2}$  obtained by fitting the data. The full decay curves were obtained by the numerical inverse Laplace transformation of eq 21 using the values of  $\kappa_D$  and  $D$ .

When  $R = 1\text{ nm}$ , the asymptotic part of the decay appeared at earlier times compared to that obtained for  $R = 0.5\text{ nm}$ . By further increasing the value of the closest separation distance of the pair denoted by  $R$ , the onset time of asymptotic decay decreases. The overall decay curves depend crucially on  $R$  in the presence of Coulomb interaction.

Under Coulomb interaction, geminate carriers are bound and the binding energy is larger as  $R$  decreases. The diffusive motion is suppressed and the initial decay follows the reaction kinetics between immobile pair of carriers for longer period compared to that in the absence of Coulomb interaction. By decreasing  $R$ , the attractive Coulomb interaction is increased at  $R$  and clearer transition from the static reaction to the diffusion-controlled kinetics is expected. As a result, the decay will become sharper by decreasing  $R$ . On the contrary, by increasing  $R$ , the decay is smoothed.

When  $r_0 = R = 5\text{ nm}$  and  $r_0 = R = 10\text{ nm}$ ,  $D = 1.1 \times 10^{-5}\text{ cm}^2/\text{s}$ , and  $D = 2.3 \times 10^{-5}\text{ cm}^2/\text{s}$  are estimated from the asymptotic decay using eqs 26 and 27 and  $\beta = 1\text{ nm}^{-1}$ , respectively. The values of the diffusion coefficient were slightly larger than that estimated when  $R = 0.5\text{ nm}$ . Judging from Figure 7,  $R \geq 5\text{ nm}$  is estimated. Relatively large separation distance indicates that carriers migrate among trap states by repeating thermal detrapping to conducting states and trapping rather than lattice random walks. Although we analyzed the experimental data by assuming tunneling, the similar decay curves could be obtained by assuming other forms of distant dependent recombination assisted by thermal excitation. Indeed, the value of diffusion constant can be estimated using eq 36 with  $N_i(r_0) = 1$  and the derivation of eq 36 does not

necessarily require the exponential distance dependence of the intrinsic recombination rate.

In conclusion of this section, we were able to estimate the diffusion coefficient of carriers in  $\text{LaTiO}_2\text{N}$  even under the effect of Coulomb interaction from the slow asymptotic decay. The value of the diffusion coefficient is estimated to be  $D \sim 1 \times 10^{-5} \text{ cm}^2/\text{s}$ .<sup>33</sup> The onset-time of asymptotic decay depends on the strength of Coulomb interaction and the closest separation distance of an electron–hole pair. By analyzing the overall decay, it is suggested that carriers migrate among trap states and the separation distance of traps could be much larger than the lattice spacing.

The migration of a carrier among trap states can be regarded as random walks under the influence of the attractive Coulomb potential from the counter carrier. The closest separation distance of an electron–hole pair could be too large for tunneling. The carrier detrapped from trap states can either be trapped again or recombine with the counter carrier. The intrinsic recombination rate actually represents the effective rate that the carrier detrapped from a trap state transfers through conducting states and recombines with the counter carrier. In experiments, wavelengths of excitation light pulses and the probe light were altered and the results indicated the presence of trap states.<sup>8,9</sup> By analyzing the ns-time profile of absorbance with a theory taking into account the Coulomb interaction and diffusion, the experimental results were reasonably interpreted on the basis of the trap states; the long-lived carriers migrate among trap states with slow detrapping rate and detrapped carriers could recombine to the counter carrier. As a result, the absorbance by survived carriers decays.

The measured diffusion coefficient reflects the rates of thermal detrapping of carriers from trap states rather than the intrinsic carrier transport in the conducting states. If the typical separation distance between traps could be characterized by the smallest separation distance between geminate carriers, the separation distance between traps could be at least 5 nm. The results indicate that the presence of traps significantly reduces the diffusion coefficients; the photocatalytic activity could be limited by the carriers close to the surface within the estimated separation distance.

**Implication to Increase the Density of Remaining Carriers.** We schematically show our theoretical interpretation on the experimental results of LTON photocatalyst in Figure 8.

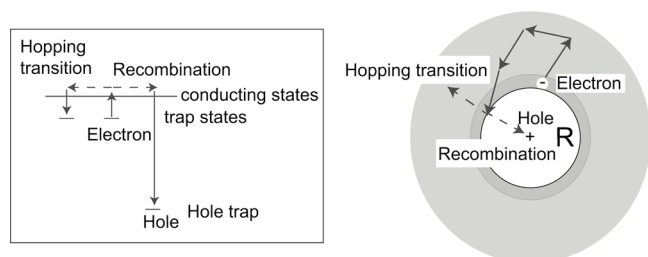


**Figure 8.** Initial distance between an electron and a hole is assumed to be  $R$ . The strength of Coulomb interaction between an electron and a hole is indicated by gray levels. The carriers execute random walks outside the spherical region of radius  $R$  by repeated detrapping, transition through conducting states and trapping. When the separation distance between an electron and a hole is  $R$ , a detrapped electron transports to either a site occupied by a hole and removes a hole by recombination or another trapping site and is trapped again.

The carriers execute random walks outside the spherical region of radius  $R$  by repeated detrapping, transition through conducting states and trapping. When the separation distance between an electron and a hole is  $R$ , a detrapped electron transports to either a site occupied by a hole and removes a hole by recombination or another trapping site and is trapped again.

The closest separation distance between geminate carriers could be an effective separation distance between trap states due to defects. The density of remaining carriers survived from geminate recombination is called the escape probability and should be correlated with the defect density. The separation distance denoted by  $R$  can be inversely proportional to the cubic root of the defect density. Using the relation between  $R$  and the defect density, the relation between the escape probability and the defect density can be obtained. The result indicates how the escape probability will be increased by decreasing the defect density. In this subsection, we estimate the escape probability when  $R$  is increased to  $R_t$  by decreasing the defect density.

In the preceding subsection, the escape probability was obtained as 0.047 by analyzing the experimental data. In the below, the closest separation distance obtained by analyzing the experimental data is denoted by  $R$  and are assumed to be 5–10 nm. The closest separation distance will be increased from  $R$  by reducing the defects and it will be denoted by  $R_t$ .

Since the precise distance dependence of recombination rate is not known for the transition of electron to the hole trap site through conducting states, we consider the case that reaction takes place with the rate given by  $k_L$  when the distance between an electron and a hole is equal to  $R_t$ . Mathematically, the rate can be expressed by eq 37, where  $R_t$  is substituted for  $R$ .

The escape probability denoted by  $S_\infty(R_t)$  is given by<sup>22,28</sup>

$$S_\infty(R_t) = \frac{1}{1 + k_L [\exp(|r_c|/R_t) - 1] / (4\pi D |r_c|)} \quad (38)$$

When the carriers transport by repeated detrapping and trapping transition through conducting states, the diffusion coefficient is proportional to the square of the effective distance between trap states. By assuming that the effective distance between traps is proportional to  $R_t$ , we set  $D \sim R_t^2$  in eq 38. The results are shown in Figure 9.

The results for  $R_t/R = 1$  is equal to the escape probability obtained by analyzing the experimental data. The results for  $R = 5 \text{ nm}$  and  $R = 10 \text{ nm}$  indicated by the solid and dashed lines are almost the same in the figure and will not be distinguished in the below. The results shown in Figure 9 can be interpreted

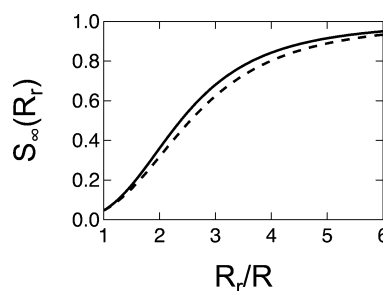


**Figure 9.** Escape probability denoted by  $S_\infty(R_t)$  as a function of  $R_t/R$ . The solid line and dashed line indicate the results when  $R = 5 \text{ nm}$  and  $R = 10 \text{ nm}$ , respectively.  $R_t$  is inversely proportional to  $n_t^{1/3}$ , where  $n_t$  is the defect density.



as the relation between the escape probability and the defect density. The effective distance between trap states could be inversely proportional to the cubic root of the defect density. For example, if the defect density is reduced to half, we have  $R_t/R = 1.26$  from  $2^{1/3} = 1.26$  and the escape probability will be almost the same as that for  $R_t/R = 1$ . On the other hand, if the defect density is reduced to one-tenth, we have  $R_t/R = 2.15$  and the escape probability is estimated to be increased to 0.4 from 0.047.

## ■ GENERALIZATION TO DISPERSIVE TRANSPORT

In this section, we consider the case where diffusion is not normal but dispersive characterized by the time evolution of mean-square displacements,  $\langle r^2 \rangle \sim t^\alpha$ . If the diffusion is dispersive, the carriers migrate slowly and the characteristic time of jumps is absent. The anomalous diffusion can be studied by fractional Fokker–Planck equation. The absence of characteristic time can be obtained by assuming activated release of carriers and an exponential distribution of activation energy expressed by  $\exp[-E/(k_B T_0)]/(k_B T_0)$ . In this case, we obtain  $\alpha = T/T_0$ .<sup>14</sup>

Previously, we have shown that electron-hole geminate recombination by tunneling under the dispersive diffusion can be studied approximately using the fractional diffusion equation with the effective sink term given by  $k(r)^\alpha$ , though in the absence of Coulomb interaction.<sup>10,34</sup> The Coulomb interaction can be taken into account using the fractional Fokker–Planck equation.<sup>35,36</sup> The effective reactivity under the dispersive transport is given by,  $k_\alpha(r) = k_0^\alpha \exp(-2\alpha\beta r)$ ,<sup>10</sup> and the approximate equation obtained previously using the fractional diffusion equation can be generalized using the Laplace transformation of the fractional Fokker–Planck equation as

$$s\hat{S}(r, s) - 1 = s^{1-\alpha} \left[ D_\alpha \frac{1}{r^2} e^{U(r)} \frac{\partial}{\partial r} r^2 e^{-U(r)} \frac{\partial}{\partial r} - k_0^\alpha \exp(-2\alpha\beta r) \right] \hat{S}(r, s) \quad (39)$$

with the reflecting boundary condition given by eq 22.

By noticing that the inverse Laplace transformation of  $s^{\alpha/2-1}$  is  $1/[\Gamma(1-\alpha/2)t^{\alpha/2}]$ , the solution can be obtained by multiplying  $(\pi t/[\Gamma(1-\alpha/2)t^{\alpha/2}])^{1/2}$  to eqs 15 and 16 and substituting  $D$  by  $D_\alpha$ ,  $k_0$  by  $k_0^\alpha$ , and  $\beta$  by  $\alpha\beta$ . For example, eq 16 is generalized to

$$S_p(R, t) = 1 - \frac{\kappa_D^{(\alpha)} K_{\alpha,p}}{1 + \kappa_D^{(\alpha)} K_{\alpha,c}} + \frac{\kappa_D^{(\alpha)} K_{\alpha,c}}{[1 + \kappa_D^{(\alpha)} K_{\alpha,c}]^2} \times \frac{|r_c|}{\Gamma(1-\alpha/2)\sqrt{D_\alpha t^\alpha}} \quad (40)$$

where we have defined  $\kappa_{\alpha,D}$ ,  $K_{\alpha,p}$ , and  $K_{\alpha,c}$  as

$$\kappa_{\alpha,D} = \frac{k_0^\alpha |r_c|^2}{D_\alpha} \quad (41)$$

$$K_{\alpha,p} = \frac{1}{|r_c|^3} \int_0^\infty r^2 dr \exp(-2\beta ar) [\exp(|r_c|/r) - 1] \quad (42)$$

$$K_{\alpha,c} = \frac{1}{|r_c|^3} \int_0^\infty r^2 dr \exp(-2\beta ar) \exp(|r_c|/r) \quad (43)$$

The exponent of the asymptotic decay of the survival probability is given by  $-\alpha/2$  instead of  $-1/2$ . The amplitude of the asymptotic decay is given in terms of the effective

intrinsic recombination rate scaled by  $\alpha$ . The distance dependence is wide ranged by the scaling.

Previously, the asymptotic power law decay with the exponent given by  $\alpha/2 + 1$  was shown without taking into account the Coulomb interaction and the theory is applied to analyze photoluminescence decay in amorphous semiconductors.<sup>7,10</sup>

In experiments, the samples of a-Si:H were excited with weak light pulses at the absorption edge of energy around 2.0 eV. The photoluminescence was observed at the peak energy, 1.22–1.35 eV. The transient photoluminescence was measured at various temperatures. The photoluminescence is proportional to the time change of the survival probability and can be theoretically obtained from

$$PL_p(R, t) = -\frac{\partial S_p(R, t)}{\partial t} = \frac{\alpha |r_c| \kappa_D^{(\alpha)} K_{\alpha,c}}{2\Gamma(1-\alpha/2)[1 + \kappa_D^{(\alpha)} K_{\alpha,c}]^2 \sqrt{D_\alpha} t^{\alpha/2+1}} \quad (44)$$

apart from the proportional constant. In the photoluminescence experiments, the information on the ultimate survival probability is lost.  $\alpha$  was related to the typical depth expressed by  $k_B T_0$  of an exponential distribution of density of states of band tails and the temperature  $T$  as  $\alpha = T/T_0$ .<sup>1,7,10,37</sup> Here, we show that the exponent is not affected by the Coulomb interaction. For a contact reaction, the same exponent was derived using percolation approach.<sup>37</sup>

## ■ CONCLUSIONS

In this manuscript, we mainly studied the asymptotic decay of pair survival probability. The initial time dependence is affected by the initial separation and the distance dependence of the intrinsic recombination rate. In contrast, the asymptotic decay is less affected by these factors and exhibits the power law decay described by  $t^{-1/2}$ .<sup>1,6</sup> The long time asymptotic decay is caused by diffusional motion. Although the asymptotic time dependence is not affected by the distance dependence of the intrinsic recombination rate, the amplitude of the decay can be largely affected by the distance dependence when the geminate charge carriers are generated deep inside the region under the influence of intrinsic recombination reaction.

In the presence of Coulomb interaction, the analytical exact solution for the pair survival probability is not known in particular when the intrinsic recombination rate is long-ranged. On the other hand, recombination of electron and hole pairs under the influence of Coulomb interaction is fundamental processes of charge separation in semiconductors used for photovoltaic solar cells and photocatalytic activities. If the amplitude of the asymptotic decay can be expressed analytically, the expression can be used to estimate the diffusion coefficient and the intrinsic recombination rate from the measurements of transient decay of carriers using weak excitation light pulses. The weak excitation light is required to suppress the bulk recombination. Moreover, when the charge pair is generated by the light pulse with the smallest possible photon energy, the initial separation of the pair is almost equal to the closest separation distance for the tunneling recombination. In experiments, such measurements can be realized using band-edge excitations with weak light intensities. Theoretically, if the initial separation is equal to the closest possible separation of an electron-hole pair, the analytical approximate solutions can be quite simplified even under the Coulomb interaction.

In this manuscript, we have obtained analytical expressions of the long time asymptotic decay using Padé approximant and by assuming that the initial separation is equal to the closest possible separation of an electron-hole pair. Then, we closely study how the estimated values of diffusion coefficients obtained from the asymptotic decay can be affected by the initial distance and the distance dependence of the intrinsic recombination rate. We pointed out that the estimated values of diffusion coefficients depend on the initial distance if the reaction is long-ranged beyond the range of Onsager radius. The dependence on the initial distance occurs because the diffusional flow under the Coulomb interaction interfaces with long-range reactivity. Otherwise, we can ignore the dependence on the initial distance.

For contact reactions expressed by eq 37, the results of Padé approximant is known to be exact. In this sense, eq 15 should reproduce the exact result for contact reactions but eq 16 is not the same as the exact result though very similar.<sup>22,28</sup> The original Padé approximant involves the double spacial integration. In contrast to eq 15, eq 16 is expressed only by single spacial integration. The reason that eq 16 does not reproduce the exact results for contact reactions is due to the introduction of the simplification to avoid the double integration.

We have applied eq 11 to the kinetics in LaTiO<sub>2</sub>N (LTON) solid photocatalyst measured using time-resolved diffuse reflectance spectroscopy with the band-edge excitations to estimate the diffusion coefficients of carriers.<sup>9</sup> The diffusion coefficient of carriers in LTON is estimated from the asymptotic decay of experimental data. The onset time of asymptotic decay is sensitive to the closest separation distance denoted by  $R$  in the presence of Coulomb interaction. The overall decay obtained from numerical calculations using eq 21 was compared to the experimental decay profile. The value of  $R$  thus estimated was in nm scales and much larger than the lattice spacing of sub-nm scales. The results indicate the recombination of carriers by thermal detrapping from traps and  $R$  might be related to the typical distance between traps. Both the small value of the diffusion coefficient and the separation distance of nm scales suggest the difficulty of carriers generated deep inside the bulk to reach the surface without trapping and importance of reducing defects to improve the photocatalytic activity of LTON. The effect of reducing defects on the density of remaining carriers is quantitatively discussed.

Finally, we studied the case where diffusion is not normal but dispersive. When carriers migrate among traps and the release of carriers from traps is an activation process with an exponential distribution of activation energy,<sup>14</sup> the mean square displacements of carriers in the absence of reaction can be expressed as  $\langle r^2 \rangle \sim t^\alpha$ . Previously, the asymptotic decay of the survival probability was approximately obtained for geminate tunneling recombination under the dispersive transport by ignoring the Coulomb interaction.<sup>10,11</sup> We have generalized the result by explicitly taking into account the Coulomb interaction. The effective distance dependence of the intrinsic recombination rate became long-ranged under the dispersive transport compared to that under the normal diffusion. The amplitude of the asymptotic decay was expressed by a coupled function between the long-ranged reactivity and the Coulomb interaction.

## AUTHOR INFORMATION

### Corresponding Author

\*E-mail: k-seki@aist.go.jp.

### Notes

The authors declare no competing financial interest.

## ACKNOWLEDGMENTS

This work is supported by “Research Project for Future Development: Artificial Photosynthetic Chemical Process (ARPCChem)” (METI/NEDO, Japan: 2012–2022).

## REFERENCES

- (1) Street, R. A. Luminescence and Recombination in Hydrogenated Amorphous Silicon. *Adv. Phys.* **1980**, *34*, 593–676.
- (2) Zhang, Z.; Wang, C.; Zakaria, R.; Ying, J. Y. Role of Particle Size in Nanocrystalline TiO<sub>2</sub>-Based Photocatalysts. *J. Phys. Chem. B* **1998**, *102*, 10871–10878.
- (3) Pope, M.; Swenberg, C. E. *Electronic Processes in Organic Crystals and Polymers*; Oxford University Press: New York, 1999.
- (4) Cichos, F.; von Borczyskowski, C.; Orrit, M. Power-Law Intermittency of Single Emitters. *Curr. Opin. Colloid Interface Sci.* **2007**, *12*, 272–284.
- (5) Borsenberger, P. M.; Weiss, D. S. *Organic Photoreceptors for Imaging Systems*; Marcel Dekker: New York, 1993.
- (6) Noolandi, J.; Hong, K. M.; Street, R. A. A Geminate Recombination Model for Photoluminescence Decay in Plasma-Deposited Amorphous Si:H. *Solid State Commun.* **1980**, *34*, 45–48.
- (7) Seki, K.; Murayama, K.; Tachiya, M. Dispersive Photoluminescence Decay by Geminate Recombination in Amorphous Semiconductors. *Phys. Rev. B* **2005**, *71*, 235212.
- (8) Hisatomi, T.; Minegishi, T.; Domen, K. Kinetic Assessment and Numerical Modeling of Photocatalytic Water Splitting toward Efficient Solar Hydrogen Production. *Bull. Chem. Soc. Jpn.* **2012**, *85*, 647–655.
- (9) Singh, R. B.; Matsuzaki, H.; Suzuki, Y.; Seki, K.; Minegishi, T.; Hisatomi, T.; Domen, K.; Furube, A. Trapped State Sensitive Kinetics in LaTiO<sub>2</sub>N Solid Photocatalyst with and without Cocatalyst Loading. *J. Am. Chem. Soc.* **2014**, *136*, 17324–17331.
- (10) Seki, K.; Wojcik, M.; Tachiya, M. Dispersive-Diffusion-Controlled Distance-Dependent Recombination in Amorphous Semiconductors. *J. Chem. Phys.* **2006**, *124*, 044702.
- (11) Seki, K.; Shushin, A. I.; Wojcik, M.; Tachiya, M. Specific Features of the Kinetics of Fractional-Diffusion Assisted Geminate Reactions. *J. Phys.: Condens. Matter* **2007**, *19*, 065117.
- (12) Shushin, A. I. Effect of Interparticle Interaction on Kinetics of Geminate Recombination of Subdiffusing Particles. *J. Chem. Phys.* **2008**, *129*, 114509.
- (13) Hong, K. M.; Noolandi, J.; Street, R. A. Theory of Radiative Recombination by Diffusion and Tunneling in Amorphous Si:H. *Phys. Rev. B* **1981**, *23*, 2967–2976.
- (14) Scher, H.; Montroll, E. W. Anomalous Transit-Time Dispersion in Amorphous Solids. *Phys. Rev. B* **1975**, *12*, 2455–2477.
- (15) Pfister, G.; Scher, H. Dispersive (non-Gaussian) Transient Transport in Disordered Solids. *Adv. Phys.* **1978**, *27*, 747–798.
- (16) Rice, S. A. *Diffusion-Limited Reactions*, *Comprehensive Chemical Kinetics*; Elsevier: Amsterdam, 1985; Vol. 25; Final expressions contain typographical errors.
- (17) Rice, S.; Butler, P.; Pilling, M. J.; Baird, J. A Solution of the Debye-Smoluchowski Equation for the Rate of Reaction of Ions in Dilute Solutions. *J. Chem. Phys.* **1979**, *70*, 4001–4007. Final expressions contain typographical errors.
- (18) Lee, S.; Son, C. Y.; Sung, J.; Chong, S. Propagator for Diffusive Dynamics of an Interacting Molecular Pair. *J. Chem. Phys.* **2011**, *134*, 121102.
- (19) Traytak, S. On the Solution of the Debye-Smoluchowski Equation with a Coulomb Potential. III. The Case of a Boltzmann Initial Distribution and a Perfectly Absorbing Sink. *Chem. Phys.* **1991**, *154*, 263–280.

- (20) Weiss, G. H. A Perturbation Analysis of the Wilemski-Fixman Approximation for Diffusion Controlled Reactions. *J. Chem. Phys.* **1984**, *80*, 2880–2887.
- (21) Abramowitz, M.; Stegun, I. A. *Handbook of Mathematical Functions*; Dover: New York, 1972.
- (22) Sano, H.; Tachiya, M. Partially Diffusion-Controlled Recombination. *J. Chem. Phys.* **1979**, *71*, 1276–1282.
- (23) Barzykin, A. V.; Frantsuzov, P. A.; Seki, K.; Tachiya, M. *Advances in Chemical Physics*; John Wiley & Sons, Inc.: New York, 2003; pp 511–616.
- (24) Stehfest, H. Algorithm 368: Numerical Inversion of Laplace Transform. *Commun. ACM* **1970**, *13*, 47–49.
- (25) Stehfest, H. Remark on Algorithm 368: Numerical Inversion of Laplace Transforms. *Commun. ACM* **1970**, *13*, 624–624.
- (26) *MATHEMATICA 10.0*; Wolfram Research: Champaign, 1988.
- (27) Onsager, L. Initial Recombination of Ions. *Phys. Rev.* **1938**, *54*, 554–557.
- (28) Hong, K. M.; Noolandi, J. Solution of the Smoluchowski Equation with a Coulomb Potential. I. General Results. *J. Chem. Phys.* **1978**, *68*, 5163–5171.
- (29) Furube, A.; Asahi, T.; Masuhara, H.; Yamashita, H.; Anpo, M. Charge Carrier Dynamics of Standard TiO<sub>2</sub> Catalysts Revealed by Femtosecond Diffuse Reflectance Spectroscopy. *J. Phys. Chem. B* **1999**, *103*, 3120–3127.
- (30) Tamaki, Y.; Furube, A.; Murai, M.; Hara, K.; Katoh, R.; Tachiya, M. Direct Observation of Reactive Trapped Holes in TiO<sub>2</sub> Undergoing Photocatalytic Oxidation of Adsorbed Alcohols: Evaluation of the Reaction Rates and Yields. *J. Am. Chem. Soc.* **2006**, *128*, 416–417.
- (31) Katoh, R.; Murai, M.; Furube, A. Electron-Hole Recombination in the Bulk of a Rutile TiO<sub>2</sub> Single Crystal Studied by Sub-Nanosecond Transient Absorption Spectroscopy. *Chem. Phys. Lett.* **2008**, *461*, 238–241.
- (32) Tamaki, Y.; Hara, K.; Tachiya, R. K.; Furube, M. A. Femtosecond Visible-to-IR Spectroscopy of TiO<sub>2</sub> Nanocrystalline Films: Elucidation of the Electron Mobility before Deep Trapping. *J. Phys. Chem. C* **2009**, *113*, 11741–11746.
- (33) The diffusion coefficient was estimated to be  $2.06 \times 10^{-3} \text{ cm}^2/\text{s}$  in ref 9 obtained using Eq 11 by assuming weak reactivity. The value should be corrected to that shown here. The separation between carriers during the measurement time of 50 ns is estimated as 10 nm. The other parts of ref 9 are not influenced by the correction.
- (34) Seki, K.; Wojcik, M.; Tachiya, M. Recombination Kinetics in Subdiffusive Media. *J. Chem. Phys.* **2003**, *119*, 7525–7533.
- (35) Metzler, R.; Klafter, J. Fractional Fokker-Planck Equation, Solution, and Application. *Phys. Rep.* **2000**, *339*, 1–77.
- (36) Barkai, E.; Metzler, R.; Klafter, J. From Continuous Time Random Walks to the Fractional Fokker-Planck Equation. *Phys. Rev. E* **2000**, *61*, 132–138.
- (37) Berlin, Y. A.; Chekunaev, N. I.; Goldanskii, V. I. Geminant Electron-Cation Recombination in Disordered Solids. *J. Chem. Phys.* **1990**, *92*, 7540–7545.